Investigation of the radical product channel of the $CH_3C(O)O_2 + HO_2$ reaction in the gas phase

M. E. Jenkin,*[a] M. D. Hurley[b] and T. J. Wallington[b]

Received 22nd February 2007, Accepted 5th April 2007
First published as an Advance Article on the web 4th May 2007
DOI: 10.1039/b702757e

The reaction of $CH_3C(O)O_2$ with HO_2 has been investigated at 296 K and 700 Torr using long path FTIR spectroscopy, during photolysis of $Cl_2/CH_3CHO/CH_3OH$/air mixtures. The branching ratio for the reaction channel forming $CH_3C(O)O$, OH and O_2 (reaction (3c)) has been determined from experiments in which OH radicals were scavenged by addition of benzene to the system, with subsequent formation of phenol used as the primary diagnostic for OH radical formation. The dependence of the phenol yield on benzene concentration was found to be consistent with its formation from the OH-initiated oxidation of benzene, thereby confirming the presence of OH radicals in the system. The dependence of the phenol yield on the initial peroxy radical precursor reagent concentration ratio, $[CH_3OH]_0/[CH_3CHO]_0$, is consistent with OH formation resulting mainly from the reaction of $CH_3C(O)O_2$ with HO_2 in the early stages of the experiments, such that the limiting yield of phenol at high benzene concentrations is well-correlated with that of $CH_3C(O)OOH$, a well-established product of the $CH_3C(O)O_2 + HO_2$ reaction (*via* channel (3a)). However, a delayed source of phenol was also identified, which is attributed mainly to an analogous OH-forming channel of the reaction of HO_2 with $HOCH_2O_2$ (reaction (17c)), formed from the reaction of HO_2 with product HCHO. This was investigated in additional series of experiments in which Cl_2/CH_3OH/benzene/air and Cl_2/HCHO/benzene/air mixtures were photolysed. The various reaction systems were fully characterised by simulations using a detailed chemical mechanism. This allowed the following branching ratios to be determined: $CH_3C(O)O_2 + HO_2 \rightarrow CH_3C(O)OOH + O_2$, $k_{3a}/k_3 = 0.38 \pm 0.13$; $\rightarrow CH_3C(O)OH + O_3$, $k_{3b}/k_3 = 0.12 \pm 0.04$; $\rightarrow CH_3C(O)O + OH + O_2$, $k_{3c}/k_3 = 0.43 \pm 0.10$: $HOCH_2O_2 + HO_2 \rightarrow HCOOH + H_2O + O_2$, $k_{17b}/k_{17} = 0.30 \pm 0.06$; $\rightarrow HOCH_2O + OH + O_2$, $k_{17c}/k_{17} = 0.20 \pm 0.05$. The results therefore provide strong evidence for significant participation of the radical-forming channels of these reactions, with the branching ratio for the title reaction being in good agreement with the value reported in one previous study. As part of this work, the kinetics of the reaction of Cl atoms with phenol (reaction (14)) have also been investigated. The rate coefficient was determined relative to the rate coefficient for the reaction of Cl with CH_3OH, during the photolysis of mixtures of Cl_2, phenol and CH_3OH, in either N_2 or air at 296 K and 760 Torr. A value of $k_{14} = (1.92 \pm 0.17) \times 10^{-10}$ cm^3 molecule^{-1} s^{-1} was determined from the experiments in N_2, in agreement with the literature. In air, the apparent rate coefficient was about a factor of two lower, which is interpreted in terms of regeneration of phenol from the product phenoxy radical, C_6H_5O, possibly *via* its reaction with HO_2.

1. Introduction

The role played by organic peroxy radicals (RO_2) in the tropospheric degradation of hydrocarbons and other volatile organic compounds (VOC) is well documented.[1–3] Under tropospheric conditions, RO_2 radicals may have several competing reactions available, the relative rates of which are dependent both on the prevailing ambient conditions, and on the structure of the peroxy radical. The propagating reactions of RO_2 with nitric oxide (NO) play a key role in tropospheric ozone formation, through oxidising NO to NO_2, and also represent the major reactions for RO_2 under comparatively polluted conditions:

$$RO_2 + NO \rightarrow RO + NO_2 \quad (1)$$

Other reactions serve to inhibit ozone formation by competing with reaction (1), in particular the reactions of RO_2 with the hydroperoxy radical (HO_2), which gain in importance as the availability of NO_X becomes more limited:

$$RO_2 + HO_2 \rightarrow \text{products} \quad (2)$$

These reactions have also long been recognised as chain terminating reactions which therefore make a major contribution to controlling atmospheric free radical concentrations under NO_X-limited conditions.[4] Whereas radical termination

[a] *Centre for Environmental Policy, Imperial College London, Silwood Park, Ascot, Berkshire, UK SL5 7PY. E-mail: m.jenkin@imperial.ac.uk*
[b] *Research and Innovation Center, Ford Motor Company, RIC-2122 PO Box 2053, Dearborn, MI 48121-2053, USA*

via the near-exclusive formation of organic hydroperoxide products (ROOH) and O_2 is well-established for simple alkyl peroxy radicals such as CH_3O_2 and $C_2H_5O_2$,[5–8] it has recently been suggested that selected oxygenated RO_2 radicals may possess significant radical-forming channels for their reactions with HO_2, thereby lessening their impact as chain terminating processes.[8,9]

Of particular interest is the reaction of the acetyl peroxy radical ($CH_3C(O)O_2$) with HO_2. The $CH_3C(O)O_2$ radical is generated during the degradation of a large number of emitted VOC $\geq C_2$, including isoprene, and thus plays an important role in atmospheric chemistry. Evidence for the significant participation of two terminating channels of the reaction was first reported in the FTIR product study of Niki *et al.*:[10]

$$CH_3C(O)O_2 + HO_2 \rightarrow CH_3C(O)OOH + O_2 \quad (3a)$$

$$\rightarrow CH_3C(O)OH + O_3 \quad (3b)$$

The existence of channels (3a) and (3b) has since been confirmed in a number of product studies,[8,11,12] and the formation of O_3 *via* channel (3b) has been observed in kinetics studies of the reaction.[12–14] The significant participation of a radical-forming channel (3c) was first suggested in the FTIR/HPLC product study of Hasson *et al.*,[8]

$$CH_3C(O)O_2 + HO_2 \rightarrow CH_3C(O)O + OH + O_2 \quad (3c)$$

primarily to explain the formation of a significant yield of CH_3OOH, which can be generated from the subsequent chemistry of $CH_3C(O)O$:

$$CH_3C(O)O \rightarrow CH_3 + CO_2 \quad (4)$$

$$CH_3 + O_2(+M) \rightarrow CH_3O_2(+M) \quad (5)$$

$$CH_3O_2 + HO_2 \rightarrow CH_3OOH + O_2 \quad (6)$$

Accordingly, they derived a branching ratio of $k_{3c}/k_3 = 0.40 \pm 0.16$, with theoretical support for the participation of channel (3c) being reported subsequently.[9] This conclusion has recently been challenged by Le Crane *et al.*,[15] who reported a re-evaluation of the results of the flash photolysis/UV absorption kinetics study of Tomas *et al.*,[14] from the same laboratory, and the results of new experiments in which benzene was added to the system to scavenge any OH radicals generated. Based primarily on analysis of UV absorption traces at 290 nm (where the product hydroxycyclohexadienyl radical absorbs) Le Crane *et al.*[15] derived an upper limit of $k_{3c}/k_3 < 0.1$. Theoretical support for the non-participation of channel (3c) was also reported.

In the present study, reaction (3) has been investigated at 296 K and 700 Torr using long path FTIR spectroscopy, during photolysis of $Cl_2/CH_3CHO/CH_3OH$/air mixtures, the same basic chemical system employed by both Hasson *et al.*[8] and Le Crane *et al.*[15] Similarly to Le Crane *et al.*, the formation of OH radicals in the system has been investigated by addition of benzene to scavenge variable proportions of OH, but with the subsequent formation of phenol used as the primary diagnostic for OH radical formation. Additional experiments using Cl_2/CH_3OH/air and Cl_2/HCHO/air mixtures have also been carried out to allow full characterisation of OH sources in the $Cl_2/CH_3CHO/CH_3OH$/air system.

2. Experimental

All experiments were performed in the Ford 140 L Pyrex chamber, interfaced with a Mattson Sirius 100 FTIR spectrometer, which is described in detail elsewhere.[16] The chamber is equipped with 22 fluorescent blacklamps (GE F40BLB), emitting near UV radiation in the range 300–450 nm. Radical generation was initiated by the photolysis of Cl_2, with $CH_3C(O)O_2$ and HO_2 radicals formed from the subsequent reaction of Cl atoms with CH_3CHO and CH_3OH, respectively, by the following well-established mechanisms:

$$Cl_2 + h\nu \rightarrow Cl + Cl \quad (7)$$

$$Cl + CH_3CHO \rightarrow CH_3CO + HCl \quad (8)$$

$$CH_3CO + O_2(+M) \rightarrow CH_3C(O)O_2(+M) \quad (9)$$

$$Cl + CH_3OH \rightarrow CH_2OH + HCl \quad (10)$$

$$CH_2OH + O_2 \rightarrow HCHO + HO_2 \quad (11)$$

Benzene was added to the reaction mixtures to scavenge variable proportions of OH radicals generated in the system. Benzene was selected because, unlike CH_3CHO and CH_3OH, it reacts slowly with Cl ($k = 1.3 \times 10^{-16}$ cm^3 molecule^{-1} s^{-1} [17]), but comparatively rapidly with OH ($k_{12} = 1.22 \times 10^{-12}$ cm^3 molecule^{-1} s^{-1} [18]). The formation of phenol from the OH-initiated oxidation of benzene (reactions (12) and (13)) was used as the primary diagnostic for OH radical formation, the reported yield of phenol being (53.1 ± 6.6)%:[19]

$$OH + C_6H_6(+M) \rightarrow HOC_6H_6(+M) \quad (12)$$

$$HOC_6H_6 + O_2 \rightarrow C_6H_5OH + HO_2 \quad (13)$$

Infra-red spectra of reagents and products were derived from 32 co-added interferograms with a spectral resolution of 0.25 cm^{-1}, and an analytical path length of 27.1 m. All experiments were carried out at 296 (±2) K and 700 Torr total pressure of air.

The organic reagents, CH_3CHO ($\geq$ 99.5%), CH_3OH ($\geq$ 99.9%) and benzene ($\geq$ 99.8%) were obtained from Aldrich Chemical Company, as were samples of the oxidation products phenol, HCHO (>95%), $CH_3C(O)OH$ (>99.99%) and $CH_3C(O)OOH$ ($\geq$ 32% in $CH_3C(O)OH$). Cl_2 and air were obtained from Michigan Airgas at research grade purity. Reference spectra were obtained by expanding calibrated volumes into the chamber. Unless otherwise specified, all quoted errors are two standard deviations.

3. Results and discussion

3.1 Characterisation of phenol removal in the system

Determination of the phenol formation yields during the $Cl_2/CH_3CHO/CH_3OH$/benzene/air experiments requires its losses in the system to be well characterised and accounted for in the analysis. Phenol reacts rapidly with Cl atoms

Table 1 Summary of experimental conditions employed to characterise the loss of phenol in the system (see Section 3.1)

Run	$[Cl_2]_0$/ mTorr	$[CH_3CHO]_0$/ mTorr	$[CH_3OH]_0$/ mTorr	$[Phenol]_0$/ mTorr	Diluent
A1	103	0	103	2.9	Air
A2	229	0	11.6	2.2	N_2
A3	107	0	99.1	2.8	N_2
A4	105	0	100	2.9	Air
A5	100	15.0	99.0	3.1	Air
A6	103	0	7.8	3.1	N_2

(reaction (14)), and it is therefore important to quantify its associated removal under the experimental conditions employed. Because reaction (14) is known to produce phenoxy radicals,[20] the possibility also exists that phenol may be reformed from its reaction with species containing labile hydrogen atoms, in particular with HO_2 (reaction (15)):

$$Cl + C_6H_5OH \rightarrow HCl + C_6H_5O \qquad (14)$$

$$C_6H_5O + HO_2 \rightarrow C_6H_5OH + O_2 \qquad (15)$$

To provide information on the removal of phenol following reaction (14), a series of experiments was performed in which the loss of phenol was measured relative to CH_3OH during UV irradiation of Cl_2/phenol/CH_3OH mixtures (see Table 1). Experiments were performed in 700 Torr of either N_2 or air diluent. Experiments in N_2 provide a measure of the rate constant ratio k_{14}/k_{10}. Experiments in air lead to the formation of HO_2 radicals (*via* reaction (11)) and, if reaction of phenoxy radicals with HO_2 (or other species formed in the oxidation of CH_3OH) is significant, may lead to reformation of phenol and hence an apparent decrease in the rate constant ratio k_{14}/k_{10}. As described elsewhere,[20] there is also a slow (probably heterogeneous) reaction of Cl_2 with phenol. In the present series of experiments the loss rate of phenol when reaction mixtures were left to stand in the dark was measured before and after UV photolysis. The phenol dark loss followed first order kinetics with the observed rate (typically 0.010–0.012 min^{-1}) being consistent with previous observations in the same chamber.[20] This information was thus used to apply appropriate corrections to phenol yields in all experiments reported here.

Fig. 1 shows a plot of the decay of phenol *versus* CH_3OH observed in the photolysis experiments. Small corrections (in the range 1–3%) have been applied to the phenol data to account for its dark removal. The open symbols show data obtained in experiments in N_2 diluent. As seen from Fig. 1, variation of the initial concentration ratio $[CH_3OH]_0/[C_6H_5OH]_0$ over the range 2.5–35.4 had no discernable impact on the results. The line through the data is a linear least squares fit which gives $k_{14}/k_{10} = 3.49 \pm 0.31$. Using the recommended value of $k_{10} = 5.5 \times 10^{-11}$ cm^3 $molecule^{-1}$ s^{-1} (ref. 21) gives $k_{14} = (1.92 \pm 0.17) \times 10^{-10}$ cm^3 $molecule^{-1}$ s^{-1}. This result is in good agreement with previous determinations of $k_{14} = (1.93 \pm 0.36) \times 10^{-10}$ cm^3 $molecule^{-1}$ s^{-1} (ref. 20) and $k_{14} = (2.4 \pm 0.4) \times 10^{-10}$ cm^3 $molecule^{-1}$ s^{-1} (ref. 22).

Interestingly, as seen by comparing the data indicated by filled symbols with those indicated by the open symbols in Fig. 1,

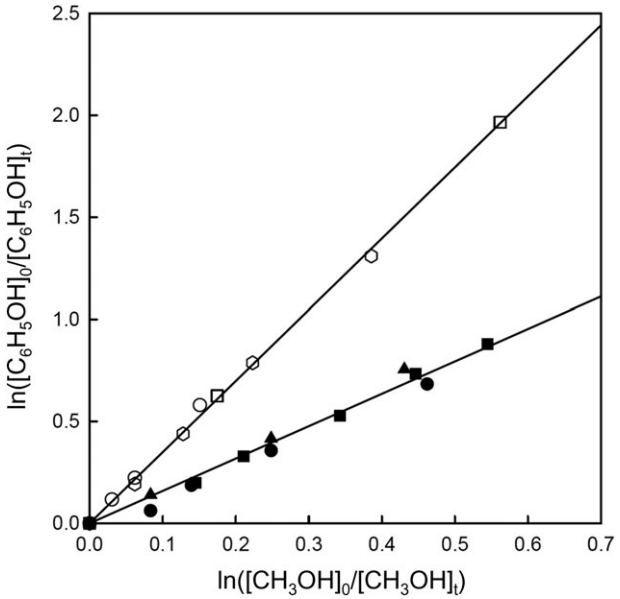

Fig. 1 Loss of phenol *versus* CH_3OH following exposure to Cl atoms in 700 Torr of N_2 (open symbols), or air (filled symbols) diluent at 296 K. $[CH_3OH]_0$ and $[C_6H_5OH]_0$ are the initial concentrations; $[CH_3OH]_t$ and $[C_6H_5OH]_t$ are concentrations at time = t. Reaction mixtures used are given in Table 1: open squares, experiment A2; open circles, experiment A3; open hexagons, experiment A6; filled squares, experiment A1; filled circles, experiment A4; and filled triangles, experiment A5.

the rate of loss of phenol observed in experiments conducted in air was approximately a factor of two lower than that observed in N_2 diluent. As indicated above, we believe that the apparent decrease in the reactivity of phenol reflects its reformation by reactions with hydrogen containing species (possibly HO_2 radicals) which are formed during the oxidation reactions which occur in air diluent. As seen from Fig. 1, addition of CH_3CHO to the CH_3OH/phenol/Cl_2 reaction mixtures had no discernable impact on the observed phenol loss rate. The line through the filled symbols in Fig. 1 is a linear least squares analysis which gives an *apparent rate constant*, k_{14obs}, describing the net loss of phenol due to reaction with Cl atoms in the system, with $k_{14obs}/k_{10} = 1.59 \pm 0.16$ and $k_{14obs} = (8.75 \pm 0.88) \times 10^{-11}$ cm^3 $molecule^{-1}$ s^{-1}. This value of k_{14obs}, obtained in air with concentrations of CH_3OH (and CH_3CHO) characteristic of those used in the subsequent experiments, was therefore used in the studies described below, either to correct the phenol yields for loss *via* reaction (14) or to calculate the reaction rate in simulations.

Our conclusion that phenol is formed in the reaction of phenoxy radicals with hydrogen containing species (possibly HO_2 radicals) may have important ramifications for atmospheric chemistry. Currently it is believed that the atmospheric fate of phenoxy radicals is reaction with NO, NO_2, and O_3.[20,23] Further work is needed to investigate the possibility that reaction with hydrogen containing species contributes to the atmospheric fate of phenoxy radicals, but such work is beyond the scope of the present investigation.

3.2 Investigation of the Cl_2/CH_3OH/benzene/air and Cl_2/HCHO/benzene/air systems

The UV photolysis of Cl_2/CH_3OH/benzene/air mixtures was initially considered, so that any sources of phenol when CH_3CHO (and therefore $CH_3C(O)O_2$) was absent from the reaction mixtures could be characterised. Three experiments were performed, covering a range of initial CH_3OH concentrations typical of those used in the experiments described in the next section (15–100 mTorr), and with *ca.* 1 Torr benzene present (see Table 2). Owing to its extremely low reactivity with Cl, benzene at this pressure scavenges $\leq 0.002\%$ of Cl atoms under the experimental conditions. However, it is sufficiently reactive with OH radicals to allow reaction (12) to compete with other reactions for OH, primarily with CH_3OH in this system:

$$OH + CH_3OH \rightarrow CH_2OH + H_2O \quad (16a)$$

$$\rightarrow CH_3O + H_2O \quad (16b)$$

leading to the formation of phenol by reaction sequence (12) and (13). Accordingly, phenol was observed in all experiments reported here in which benzene was added, with the structured infra-red band near 750 cm^{-1} allowing its sensitive and specific detection and quantification (see Fig. 2).

As shown in Fig. 3, prompt formation of HCHO as a primary product (*via* reaction sequence (10) and (11)) was observed in each of the Cl_2/CH_3OH/benzene/air experiments, with delayed formation of HCOOH and phenol also observed, characteristic of their formation resulting from subsequent reactions involving HCHO. Previous studies have demonstrated that HCOOH is generated from reactions of the $HOCH_2O_2$ radical, which is present in equilibrium with HO_2 and HCHO:[24–27]

$$HCHO + HO_2 \rightleftharpoons HOCH_2O_2 \quad (16)$$

$$HOCH_2O_2 + HO_2 \rightarrow HOCH_2OOH + O_2 \quad (17a)$$

$$\rightarrow HCOOH + H_2O + O_2 \quad (17b)$$

$$HOCH_2O_2 + HOCH_2O_2 \rightarrow HOCH_2O + HOCH_2O + O_2 \quad (18a)$$

$$\rightarrow HCOOH + HOCH_2OH + O_2 \quad (18b)$$

$$HOCH_2O + O_2 \rightarrow HCOOH + HO_2 \quad (19)$$

Under the experimental conditions, $HOCH_2O_2$ is mainly removed *via* reaction with HO_2 (reaction (17)), such that this reaction provides the major route to HCOOH formation. To test established understanding of this chemistry, the system was simulated using the explicit mechanism in Table 3, which includes the above reaction sequence. This provided an acceptable description of the formation of HCHO and HCOOH in the system. Sensitivity tests demonstrated that use of the branching ratios $k_{17a}/k_{17} = k_{17b}/k_{17} = 0.5$ allowed a good description of the formation of HCOOH relative to CH_3OH removed (as presented in Fig. 3), in good agreement with the values of $k_{17a}/k_{17} = 0.6$ and $k_{17b}/k_{17} = 0.4$, reported by Burrows *et al.*,[27] and recommended by Atkinson *et al.*[21] Some formation of phenol was also simulated, by virtue of OH production from the reaction of Cl atoms with $HOCH_2OOH$, formed from channel (17a),

$$Cl + HOCH_2OOH \rightarrow HOCHOOH + HCl \quad (20)$$

$$HOCHOOH \rightarrow HCOOH + OH \quad (21)$$

this reaction sequence being defined in the mechanism by analogy with known reactions of CH_3OOH and CH_2OOH.[36] As shown in Fig. 3, however, this source was insufficient to account for the observed phenol formation, even if reaction (17) was assumed to proceed entirely *via* channel (17a). It is therefore necessary to invoke an additional OH-forming channel of reaction (17),

$$HOCH_2O_2 + HO_2 \rightarrow HOCH_2O + OH + O_2 \quad (17c)$$

which also produces HCOOH from the subsequent reaction (19) of $HOCH_2O$. The reaction (17) branching ratios were

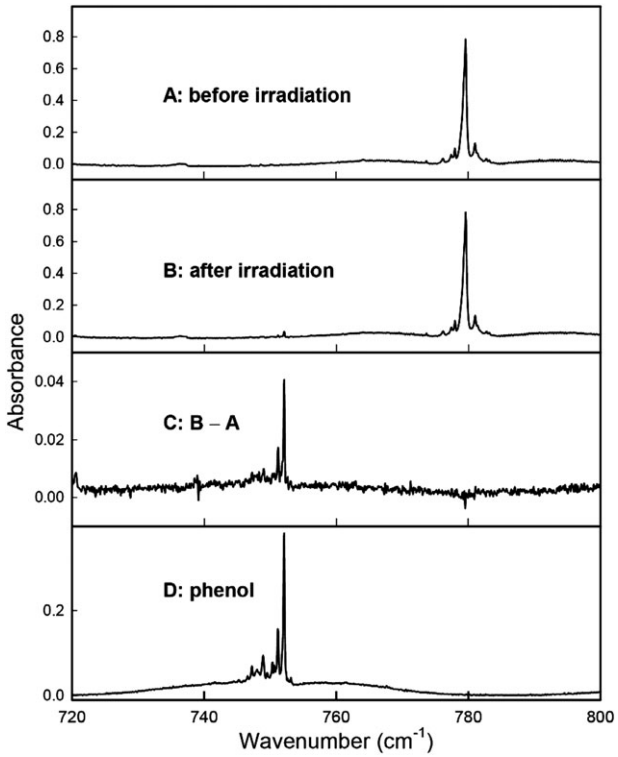

Fig. 2 IR spectra obtained before (A) and after (B) a 55 sec irradiation of the $Cl_2/CH_3CHO/CH_3OH$/benzene/air mixture in experiment C12. The feature at 779 cm^{-1} is attributable to benzene. Panel C shows the difference spectrum. A reference spectrum of phenol is given in panel D.

Table 2 Summary of experimental conditions employed for "Cl_2/CH_3OH/benzene/air" and "Cl_2/HCHO/benzene/air" experiments (see Section 3.2)

Run	$[Cl_2]_0$/ mTorr	$[CH_3OH]_0$/ mTorr	$[HCHO]_0$/ mTorr	$[Benzene]_0$/ mTorr
B1	101	99.7	0	1000
B2	101	49.3	0	1020
B3	101	15.7	0	1000
B4	100	0	10.1	1000

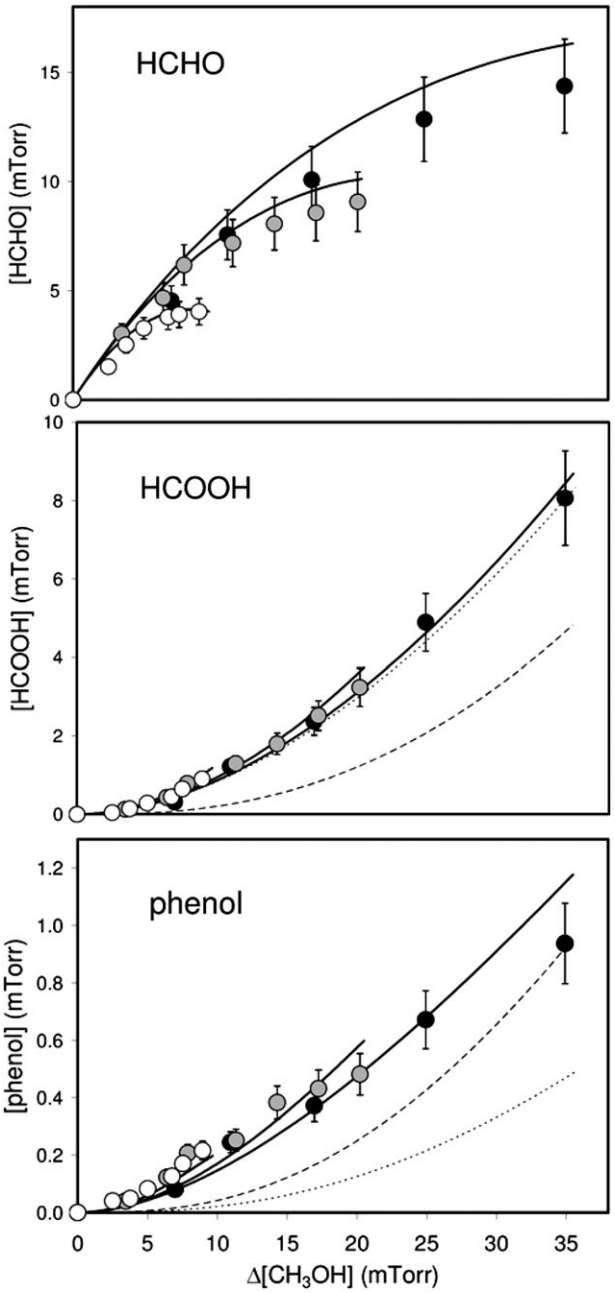

Fig. 3 Formation of HCHO, HCOOH and phenol relative to CH_3OH lost during the photolysis of Cl_2/CH_3OH/benzene/air mixtures. Black points, experiment B1; grey points, experiment B2; open points, experiment B3. Solid lines are simulations using mechanism in Table 3 with $k_{17a}/k_{17} = 0.5$, $k_{17b}/k_{17} = 0.3$ and $k_{17c}/k_{17} = 0.2$. Dotted and dashed lines show simulated phenol formation for experiment B1 when $k_{17a}/k_{17} = k_{17b}/k_{17} = 0.5$, and when $k_{17a}/k_{17} = 1$, respectively. Phenol data have been corrected for dark removal (see text).

varied to optimise the agreement between the simulated and observed formation of HCOOH and phenol in all three experiments, leading to value of $k_{17b}/k_{17} = 0.30 \pm 0.06$ and $k_{17c}/k_{17} = 0.20 \pm 0.05$, with the balance assumed to proceed *via* channel (17a). The combined branching ratio of the HCOOH-forming channels (reactions (17b) and (17c)) is thus entirely consistent with that reported for channel (17b) by Burrows *et al*. (1989), which was based on observed formation of HCOOH.

To confirm this optimized description of the system, a Cl_2/HCHO/benzene/air photolysis experiment was also carried out (see Table 2). In this system, HO_2 radicals are generated from the reaction of Cl with HCHO:

$$Cl + HCHO \rightarrow HCO + HCl \qquad (22)$$

$$HCO + O_2 \rightarrow HO_2 + CO \qquad (23)$$

Because HCHO does not need to accumulate in the system, prompt formation of HCOOH and phenol occurs as a result of the chemistry described above. As shown in Fig. 4, the chemical mechanism in Table 3, along with the branching ratios for reaction (17) optimised in the CH_3OH system, provide a good description of the time dependence of HCOOH and phenol (and CO) formation. This confirms that the representation of the associated chemistry in Table 3 is well characterised, providing a sound basis for accounting for OH sources not associated with CH_3CHO chemistry in the $Cl_2/CH_3CHO/CH_3OH$/benzene/air system.

3.3 Investigation of the $Cl_2/CH_3CHO/CH_3OH$/benzene/air system

3.3.1 Analysis and interpretation of phenol formation. The reaction of $CH_3C(O)O_2$ with HO_2 (reaction (3)) was initially investigated in a series of $Cl_2/CH_3CHO/CH_3OH$/benzene/air UV photolysis experiments in which a high ratio of the peroxy radical precursor concentration, $[CH_3OH]_0/[CH_3CHO]_0 \approx 7$, was employed (see Table 4). Under these conditions, the production rate of HO_2 radicals is *ca*. 5 times greater than that of $CH_3C(O)O_2$ radicals, such that HO_2 radicals are in excess (typically by an order of magnitude under the steady state photolysis conditions applied here). Previous studies have demonstrated that $CH_3C(O)O_2$ reacts mainly with HO_2 under such conditions,[8,12] and this was also confirmed in the present study from experiments carried out for a range of $[CH_3OH]_0/[CH_3CHO]_0$ ratios, and by simulation of the system, as described further below.

Experiments were carried out with benzene present in the reaction mixtures at a series of pressures up to *ca*. 1 Torr. Similarly to above, benzene at these pressures does not interfere with the production of $CH_3C(O)O_2$ and HO_2 under the conditions employed (scavenging $\leq 0.002\%$ of Cl atoms), but is sufficiently reactive to scavenge OH radicals in competition with other reactions of OH, *i.e*., primarily its reactions with CH_3OH (reaction (16)) and CH_3CHO:

$$OH + CH_3CHO \rightarrow CH_3CO + H_2O \qquad (24)$$

Accordingly, phenol formation was observed in all experiments in which benzene was added. Unlike the results for the Cl_2/CH_3OH/benzene/air system above, however, phenol formation was observed to be prompt, such that its yields at short reaction times were considerably greater than those observed under comparable conditions in the absence of CH_3CHO. As shown in Fig. 5 (inset), the formation of phenol correlated well with the amount of CH_3CHO consumed, and its yield increased with benzene concentration in the system. To test that phenol formation was due to the OH-initiated oxidation of

Table 3 Detailed reaction mechanism and associated parameters used to simulate the Cl/CH_3OH/benzene/air, Cl/HCHO/benzene/air and Cl/CH_3CHO/CH_3OH/benzene/air photolysis experiments. The more significant reactions in the Cl/CH_3CHO/CH_3OH/benzene/air simulations are shown in bold font

	Reaction	Branching ratio	Rate coefficient [(a)]	Comment
Initiation reactions				
$Cl_2 + h\nu$	**$\rightarrow$ Cl + Cl**		7.5×10^{-4} s^{-1}	(b)
Cl + CH_3CHO (+O_2)	**$\rightarrow$ $CH_3C(O)O_2$ + HCl**		8.0×10^{-11}	(c)
Cl + CH_3OH (+O_2)	**$\rightarrow$ HCHO + HO_2 + HCl**		5.5×10^{-11}	(c)
Cl + HCHO (+O_2)	**$\rightarrow$ CO + HO_2 + HCl**		$8.1 \times 10^{-11} \exp(-34/T)$	(c)
OH + CH_3CHO (+O_2)	**$\rightarrow$ $CH_3C(O)O_2$ + H_2O**		$4.4 \times 10^{-12} \exp(365/T)$	(c)
OH + CH_3OH (+O_2)	**$\rightarrow$ HCHO + HO_2 + H_2O**		$2.85 \times 10^{-12} \exp(-345/T)$	(c)
OH + HCHO (+O_2)	**$\rightarrow$ CO + HO_2 + H_2O**		$5.4 \times 10^{-12} \exp(135/T)$	(c)
HO_2 + CH_3CHO	**$\rightarrow$ $CH_3CH(OH)O_2$**		$k_f = 4.4 \times 10^{-14}$ $k_r = 2.3 \times 10^{13} \exp(-6925/T)$ s^{-1}	(d)
HO_2 + HCHO	**$\rightarrow$ $HOCH_2O_2$**		$k_f = 9.7 \times 10^{-15} \exp(625/T)$ $k_r = 2.4 \times 10^{12} \exp(-7000/T)$ s^{-1}	(c)
RO_2 + HO_2 reactions				
HO_2 + HO_2	**$\rightarrow$ H_2O_2 + O_2**		$2.2 \times 10^{-13} \exp(600/T) + 1.9 \times 10^{-33}$ [M] $\exp(980/T)$	(e)
$CH_3C(O)O_2$ + HO_2	**$\rightarrow$ $CH_3C(O)OOH$ + O_2**	Varied (see text)	$5.2 \times 10^{-13} \exp(980/T)$	(c)
	$\rightarrow$ $CH_3C(O)OH$ + O_3			
	$\rightarrow$ $CH_3C(O)O$ + OH + O_2			
CH_3O_2 + HO_2	**$\rightarrow$ CH_3OOH + O_2**	0.9	$3.8 \times 10^{-13} \exp(780/T)$	(c)
	$\rightarrow$ HCHO + H_2O + O_2	0.1		
$HOCH_2O_2$ + HO_2	**$\rightarrow$ $HOCH_2OOH$ + O_2**	Varied (see text)	$5.6 \times 10^{-15} \exp(2300/T)$	(c)
	$\rightarrow$ HCOOH + H_2O + O_2			
	$\rightarrow$ $HOCH_2O$ + OH + O_2			
$CH_3CH(OH)O_2$ + HO_2	**$\rightarrow$ $CH_3CH(OH)OOH$ + O_2**	0.5	$5.6 \times 10^{-15} \exp(2300/T)$	(f), (g)
	$\rightarrow$ $CH_3C(O)OH$ + H_2O + O_2	0.3		
	$\rightarrow$ $CH_3CH(OH)O$ + OH + O_2	0.2		
RO_2 + RO_2 reactions				
2 $CH_3C(O)O_2$	**$\rightarrow$ 2 $CH_3C(O)O$ + O_2**		$2.9 \times 10^{-12} \exp(500/T)$	(c)
2 CH_3O_2	$\rightarrow$ 2 CH_3O + O_2	0.37	$1.03 \times 10^{-13} \exp(365/T)$	(c)
	$\rightarrow$ HCHO + CH_3OH + O_2	0.63		
2 $HOCH_2O_2$	$\rightarrow$ 2 $HOCH_2O$ + O_2	0.88	5.7×10^{-12}	(c)
	$\rightarrow$ HCOOH + $HOCH_2OH$ + O_2	0.12		
2 $CH_3CH(OH)O_2$	$\rightarrow$ 2 $CH_3CH(OH)O$ + O_2	0.88	5.7×10^{-12}	(f)
	$\rightarrow$ $CH_3C(O)OH$ + $CH_3C(OH)_2$ + O_2	0.12		
RO_2 + $R'O_2$ reactions				
$CH_3C(O)O_2$ + CH_3O_2	**$\rightarrow$ $CH_3C(O)O$ + CH_3O + O_2**	0.9	$2.0 \times 10^{-12} \exp(500/T)$	(c)
	$\rightarrow$ $CH_3C(O)OH$ + HCHO + O_2	0.1		
$CH_3C(O)O_2$ + $HOCH_2O_2$	**$\rightarrow$ $CH_3C(O)O$ + $HOCH_2O$ + O_2**	0.9	$2.0 \times 10^{-12} \exp(500/T)$	(h)
	$\rightarrow$ $CH_3C(O)OH$ + HCOOH + O_2	0.1		
$CH_3C(O)O_2$ + $CH_3CH(OH)O_2$	**$\rightarrow$ $CH_3C(O)O$ + $CH_3CH(OH)O$ + O_2**	0.9	$2.0 \times 10^{-12} \exp(500/T)$	(h)
	$\rightarrow$ $CH_3C(O)OH$ + $CH_3C(O)OH$ + O_2	0.1		
CH_3O_2 + $HOCH_2O_2$	$\rightarrow$ CH_3O + $HOCH_2O$ + O_2	0.62	1.4×10^{-12}	(i)
	$\rightarrow$ CH_3OH + HCOOH + O_2	0.19		
	$\rightarrow$ HCHO + $HOCH_2OH$ + O_2	0.19		
CH_3O_2 + $CH_3C(OH)O_2$	$\rightarrow$ CH_3O + $CH_3C(OH)O$ + O_2	0.62	1.4×10^{-12}	(i)
	$\rightarrow$ CH_3OH + $CH_3C(O)OH$ + O_2	0.19		
	$\rightarrow$ HCHO + $CH_3C(OH)_2$ + O_2	0.19		
$HOCH_2O_2$ + $CH_3C(OH)O_2$	$\rightarrow$ $HOCH_2O$ + $CH_3C(OH)O$ + O_2	0.88	5.7×10^{-12}	(i)
	$\rightarrow$ $HOCH_2OH$ + $CH_3C(O)OH$ + O_2	0.06		
	$\rightarrow$ HCOOH + $CH_3C(OH)_2$ + O_2	0.06		
RO reactions				
$CH_3C(O)O$ (decomp + O_2)	**$\rightarrow$ CH_3O_2 + CO_2**		Assumed instantaneous	(j)
CH_3O + O_2	**$\rightarrow$ HCHO + HO_2**		Assumed instantaneous	(j)
$HOCH_2O$ + O_2	**$\rightarrow$ HCOOH + HO_2**		Assumed instantaneous	(k)
$CH_3CH(OH)O$ (decomp + O_2)	**$\rightarrow$ HCOOH + CH_3O_2**		Assumed instantaneous	(l)
Cl + product reactions				
Cl + $CH_3C(O)OH$	$\rightarrow$ $CH_3C(O)O$ + HCl		2.65×10^{-14}	(c)
Cl + $CH_3C(O)OOH$	$\rightarrow$ $CH_3C(O)O_2$ + HCl		4.5×10^{-15}	(m)
Cl + H_2O_2	$\rightarrow$ HO_2 + HCl		$1.1 \times 10^{-11} \exp(-980/T)$	(n)
Cl + CH_3OOH	$\rightarrow$ HCHO + OH + HCl		5.9×10^{-11}	(c)
Cl + HCOOH (+O_2)	$\rightarrow$ CO_2 + HO_2 + HCl		1.9×10^{-13}	(c)
Cl + $HOCH_2OOH$	$\rightarrow$ HCOOH + OH + HCl		1.0×10^{-10}	(o)
Cl + $HOCH_2OH$ (+O_2)	$\rightarrow$ HCOOH + HO_2 + HCl		1.0×10^{-10}	(o)
Cl + $CH_3CH(OH)OOH$	$\rightarrow$ $CH_3C(O)OH$ + OH + HCl		1.0×10^{-10}	(o)

Table 3 (*continued*)

	Reaction	Branching ratio	Rate coefficient [(a)]	Comment
Cl + $CH_3CH(OH)OH$ (+ O_2)	→ $CH_3C(O)OH$ + HO_2 + HCl		1.0×10^{-10}	(o)
Cl + O_3	→ ClO + O_2		$2.8 \times 10^{-11} \exp(-250/T)$	(n)
ClO + HO_2	→ HOCl + O_2		$2.2 \times 10^{-12} \exp(340/T)$	(n)
OH + product reactions				
OH + $CH_3C(O)OH$	→ $CH_3C(O)O$ + H_2O		$4.2 \times 10^{-14} \exp(855/T)$	(c)
OH + $CH_3C(O)OOH$	→ $CH_3C(O)O_2$ + H_2O		3.6×10^{-12}	(p)
OH + H_2O_2	→ HO_2 + H_2O		$2.9 \times 10^{-12} \exp(-160/T)$	(e)
OH + CH_3OOH	→ CH_3O_2 + HO_2	0.65	$2.9 \times 10^{-12} \exp(190/T)$	(c)
	→ HCHO + OH + H_2O	0.35		
OH + HCOOH (+ O_2)	→ CO_2 + HO_2 + H_2O		4.5×10^{-13}	(c)
OH + $HOCH_2OOH$	→ $HOCH_2O_2$ + H_2O	0.12	3.1×10^{-11}	(q)
	→ HCOOH + OH + H_2O	0.88		
OH + $HOCH_2OH$ (+ O_2)	→ HCOOH + HO_2 + H_2O		1.1×10^{-11}	(q)
OH + $CH_3CH(OH)OOH$	→ $CH_3C(O)OH$ + OH + H_2O		6.0×10^{-11}	(q)
OH + $CH_3CH(OH)OH$ (+ O_2)	→ $CH_3C(O)OH$ + HO_2 + H_2O		2.4×10^{-11}	(q)
OH + Cl_2	→ Cl + HOCl		$3.6 \times 10^{-12} \exp(-1200/T)$	(m)
OH + CO (+ O_2)	→ CO_2 + HO_2		$1.44 \times 10^{-13} + 3.43 \times 10^{-33}$ [M]	(e)
OH + HCl	→ Cl + H_2O		$1.7 \times 10^{-12} \exp(-230/T)$	(m)
OH + O_3	→ HO_2 + O_2		$1.7 \times 10^{-12} \exp(-940/T)$	(e)
HO_2 + O_3	→ OH + 2 O_2		$2.03 \times 10^{-16} (T/300)^{4.57} \exp(693/T)$	(e)
Benzene chemistry				
OH + C_6H_6 (+O_2)	→ **C_6H_5OH + HO_2**	0.531	1.22×10^{-12}	(r)
	→ **(+O_2) → Φ-O_2**	0.469		
Φ-O_2 + HO_2	→ **Φ-OOH + O_2**		1.0×10^{-11}	(s)
Φ-O_2 + $CH_3C(O)O_2$	→ Φ-O + $CH_3C(O)O$ + O_2		1.0×10^{-11}	(s)
Φ-O_2 + CH_3O_2	→ Φ-O + CH_3O + O_2	0.5	2.0×10^{-12}	(s)
	→ Φ-OH + HCHO + O_2	0.5		
Φ-O_2 + $HOCH_2O_2$	→ Φ-O + $HOCH_2O$ + O_2	0.5	2.0×10^{-12}	(s)
	→ Φ-OH + HCOOH + O_2	0.5		
Φ-O_2 + $CH_3CH(OH)O_2$	→ Φ-O + $CH_3CH(OH)O$ + O_2	0.5	2.0×10^{-12}	(s)
	→ Φ-OH + $CH_3C(O)OH$ + O_2	0.5		
2 Φ-O_2	→ 2 Φ-O O_2		1.0×10^{-11}	(s)
Φ-O (decomp + O_2)	→ $(CHO)_2$ + HCOCH=CHCHO + HO_2		Assumed instantaneous	(t)
Cl + C_6H_5OH	→ **C_6H_5O + HCl**		8.75×10^{-11}	(u)
Cl + $(CHO)_2$ (+ O_2)	→ CO + CO + HO_2 + HCl		8.0×10^{-11}	(v)
Cl + HCOCH=CHCHO	→ products		1.0×10^{-10}	(o)
Cl + Φ-OOH	→ products		1.0×10^{-10}	(o)
Cl + Φ-OH (+ O_2)	→ $(CHO)_2$ + HCOCH=CHCHO + HO_2 + HCl		1.0×10^{-10}	(o)
OH + C_6H_5OH	→ C_6H_5O + H_2O		1.24×10^{-11}	(w)
OH + $(CHO)_2$ (+ O_2)	→ CO + CO + HO_2 + H_2O		1.1×10^{-11}	(c)
OH + HCOCH=CHCHO	→ products		5.2×10^{-11}	(x)
OH + Φ-OOH	→ products		1.0×10^{-11}	(y)
OH + Φ-OH (+ O_2)	→ $(CHO)_2$ + HCOCH=CHCHO + HO_2 + H_2O		1.0×10^{-11}	(y)

(a) Units cm^3 $molecule^{-1}$ s^{-1}, unless stated; (b) Characteristic of reaction chamber; (c) Based on IUPAC recommendation, Atkinson *et al.*[21] (http://www.iupac-kinetic.ch.cam.ac.uk/); (d) From Tomas *et al.*;[14] (e) Based on IUPAC recommendation, Atkinson *et al.*[28] (http://www.iupac-kinetic.ch.cam.ac.uk/); (f) Parameters assumed equivalent to that for analogous reaction of the structurally similar α-hydroxy peroxy radical, $HOCH_2O_2$; (g) Applied channel branching ratios based on those optimised for $HOCH_2O_2$ in the present study (see text); (h) Parameters assumed equivalent to those for $CH_3C(O)O_2$ + CH_3O_2 reaction; (i) Rate coefficient based on geometric mean of self-reaction rate coefficients of participating peroxy radicals. Branching ratios based on arithmetic mean of self-reaction branching ratios of participating peroxy radicals; (j) RO reactions occur on ≤20 μs timescale. Reaction products consistent with information in Atkinson *et al.*;[21] (k) RO reactions occur on ≤20 μs timescale. Reaction with O_2 estimated to dominate over decomposition by H atom ejection, based on Veyret *et al.*,[29] although ultimate products under experimental conditions are indistinguishable; (l) RO reactions occur on ≤20 μs timescale. $CH_3CH(OH)O$ is assumed to decompose in preference to reaction with O_2, consistent with the reported formation of HCOOH from larger α-hydroxy oxy radicals (Orlando *et al.*,[30]; Jenkin *et al.*,[31]); (m) From Crawford *et al.*;[12] (n) Based on current IUPAC recommendation (http://www.iupac-kinetic.ch.cam.ac.uk/); (o) Estimated to be rapid, on the basis of known reactivity of Cl with species containing –OOH, –OH, –CHO groups and unsaturated linkages; (p) Based on reactivity of –OOH group in CH_3OOH; (q) Based on SAR method of Kwok and Atkinson,[32] using a neighbouring group activation of 8.4 for –OOH, where appropriate, based on Saunders *et al.*;[33] (r) Based recommendation of Calvert *et al.*[18] Branching ratio for phenol (C_6H_5OH) and HO_2 formation based on Volkamer *et al.*,[19] with balance of reaction assumed to yield a complex bicyclic RO_2 radical in these simulations (see also Section 3.4); (s) Rate coefficients and branching ratios estimated on the basis of known reactions of peroxy radicals; (t) RO reactions occur on ≤20 μs timescale. Reaction products consistent with end product studies of benzene oxidation (Calvert *et al.*,[18]; Volkamer *et al.*[34]); (u) Apparent rate coefficient measured in present study, which takes account of partial phenol (C_6H_5OH) regeneration (see Section 3.1); (v) Based on known reactivity of Cl with CH_3CHO and HCHO; (w) Based on IUPAC recommendation, Atkinson *et al.*,[21] but reduced to take account of partial phenol (C_6H_5OH) regeneration on the basis of Cl-initiated investigation in the present study (see Section 3.1); (x) Based on Bierbach *et al.*[35]; (y) Estimated on the basis of known reactivity of OH with species containing –OOH and –OH groups.

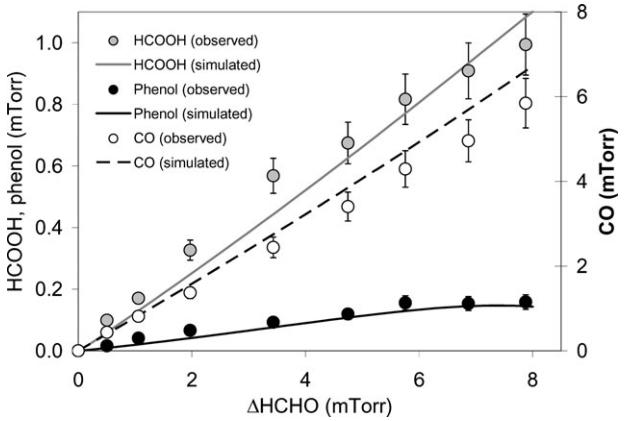

Fig. 4 Formation of CO, HCOOH and phenol relative to HCHO lost during the photolysis of Cl_2/HCHO/benzene/air mixtures (experiment B4). Displayed simulations were carried out using mechanism in Table 3 with $k_{17a}/k_{17} = 0.5$, $k_{17b}/k_{17} = 0.3$ and $k_{17c}/k_{17} = 0.2$. Phenol data have been corrected for dark removal (see text).

benzene (and not *via* some alternative oxidation mechanism), the yield of phenol, as determined from its initial formation rate, was plotted against the quantity $k_{12}[\text{benzene}]_0/(k_{12}[\text{benzene}]_0 + k_{24}[CH_3CHO]_0 + k_{16}[CH_3OH]_0)$, *i.e.*, the calculated fraction of OH reacting with benzene, hereafter denoted "f_{OH}". For this analysis, the consumption of CH_3CHO was limited to $\leq$25%, and appropriate corrections in the range *ca.* 2–20% were applied to the phenol yields to account for losses due to the processes described in Section 3.1. This constraint also served to limit the contribution to phenol formation from the $HOCH_2O_2$ chemistry described above. The resultant linear dependence (Fig. 5) confirms that phenol formation indeed arises from reaction (12) occurring in competition with the other loss routes for OH, and therefore provides a clear demonstration that OH radicals are formed in the system. The plot also indicates that *ca.* 80% of OH radicals were scavenged by reaction with benzene at the highest concentration employed (*ca.* 1 Torr), with the slope of the plot providing a measure of the limiting phenol yield under conditions when OH would react exclusively with benzene. This leads to a limiting phenol yield of 0.219 ± 0.016. Combining this value with the reported yield of phenol of 0.531 ± 0.066 from the OH-initiated oxidation of benzene,[19] provides a value of 0.41 ± 0.06 for the yield of OH radicals relative to CH_3CHO consumed at $[CH_3OH]_0/[CH_3CHO]_0 \approx 7$.

Consideration of the relative removal rates of CH_3OH and CH_3CHO provides some additional support for the production of OH radicals in the system. Fig. 6a shows a plot of the decay of CH_3CHO *versus* CH_3OH for the same series of experiments, which demonstrates that the relative removal rate depends on the concentration of benzene. At the high end of the benzene concentration range, the relative decay tends towards a value which is consistent with removal of CH_3CHO and CH_3OH predominantly by reaction with Cl atoms, the recommended ratio for the Cl atom reactions being $k_8/k_{10} = 1.46$ (ref. 21). As the concentration of benzene is reduced, the removal of CH_3CHO relative to CH_3OH is progressively enhanced, reaching a value of *ca.* 2.1 in the absence of benzene. Given that the OH reactivity of CH_3CHO relative to that of CH_3OH is much greater than for Cl, $k_{24}/k_{16} = 16.7$ (ref. 21), this observation is fully consistent with the production of OH in the system and with suppression of its concentration in the presence of benzene at the concentrations employed here.

To confirm that the production of OH results from reaction (3), the effect of varying the initial ratio of the peroxy radical precursors, $[CH_3OH]_0/[CH_3CHO]_0$, over the range zero to *ca.* 7 was also investigated (Table 4), leading to a wide variation in the relative production rates of $CH_3C(O)O_2$ and HO_2. This series of experiments was carried out with benzene present at *ca.* 1 Torr, to allow quantification of OH radical formation. In the absence of CH_3OH, there is no primary route to HO_2 formation, and $CH_3C(O)O_2$ radicals are initially removed by their self reaction:

$$CH_3C(O)O_2 + CH_3C(O)O_2 \rightarrow CH_3C(O)O + CH_3C(O)O + O_2 \quad (25)$$

As described above, the subsequent chemistry of the acetoxy radical, $CH_3C(O)O$, leads to the formation of CH_3O_2 radicals (reactions (4) and (5)), with HO_2 radicals also being generated,

Table 4 Summary of experimental conditions and yields of phenol, $CH_3C(O)OOH$ and $CH_3C(O)OH$ in $Cl_2/CH_3CHO/CH_3OH$/benzene/air experiments (see Section 3.3)

Run	$[Cl_2]_0$/ mTorr	$[CH_3CHO]_0$/ mTorr	$[CH_3OH]_0$/ mTorr	$[\text{Benzene}]_0$/ mTorr	Phenol yield[a]	$CH_3C(O)OOH$ yield[a]	$CH_3C(O)OH$ yield[a]
C1	100	14.7	100	1070	0.176 ± 0.024	0.229 ± 0.041	0.110 ± 0.012
C2	100	15.4	50.1	1050	0.157 ± 0.030	0.195 ± 0.059	0.099 ± 0.026
C3	120	15.7	0	1060	0.056 ± 0.006	0.078 ± 0.005	0.045 ± 0.010
C4	100	15.4	14.9	1030	0.093 ± 0.018	0.120 ± 0.020	0.060 ± 0.008
C5	101	15.1	75.0	1060	0.176 ± 0.028	0.222 ± 0.061	0.114 ± 0.014
C6	200	30.0	206	1060	0.138 ± 0.014	0.225 ± 0.025	0.089 ± 0.028
C7	101	15.0	100	100	0.062 ± 0.008	0.251 ± 0.030	0.104 ± 0.010
C8	100	15.0	100	0	0	0.258 ± 0.030	0.093 ± 0.018
C9	102	15.0	99.4	50.6	0.026 ± 0.006	0.221 ± 0.039	0.114 ± 0.018
C10	100	15.0	100	199	0.101 ± 0.006	0.243 ± 0.023	0.133 ± 0.014
C11	99.9	15.4	99.9	449	0.139 ± 0.016	0.266 ± 0.068	0.133 ± 0.024
C12	100	15.0	100	1010	0.177 ± 0.022	0.245 ± 0.025	0.106 ± 0.016

[a] Molar yields determined relative to CH_3CHO removed, and corrected for removal.

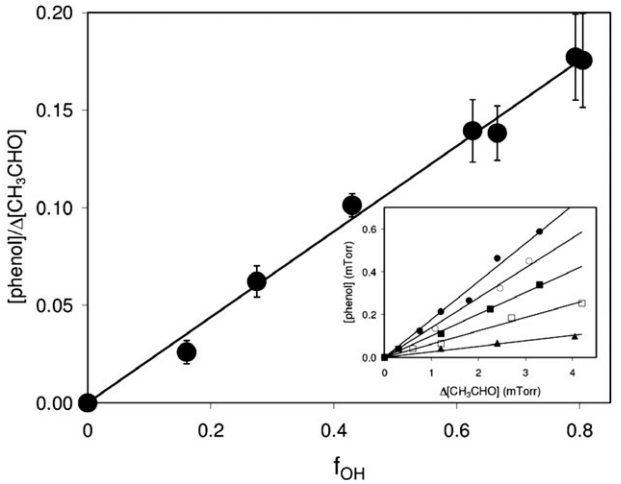

Fig. 5 Observed yield of phenol *vs.* the calculated fraction of OH scavenged by reaction with benzene (f_{OH}), in experiments with $[CH_3OH]_0/[CH_3CHO]_0 \approx 7$, with benzene added to the system at pressures up to *ca.* 1 Torr (see Table 4). Inset shows results for experiments C9 (50.6 mTorr benzene: triangles), C7 (100 mTorr benzene: open squares), C10 (199 mTorr benzene: closed squares), C11 (449 mTorr benzene: open circles) and C12 (1010 mTorr benzene: closed circles). Determination of f_{OH} based on k_{12} ($=1.22 \times 10^{-12}$ cm^3 molecule^{-1} s^{-1}) taken from the evaluation of Calvert *et al.*,[18] and k_{16} ($=9.0 \times 10^{-13}$ cm^3 molecule^{-1} s^{-1}) and k_{24} ($=1.5 \times 10^{-11}$ cm^3 molecule^{-1} s^{-1}) from the evaluation of Atkinson *et al.*[21] Phenol data have been corrected for removal (see text).

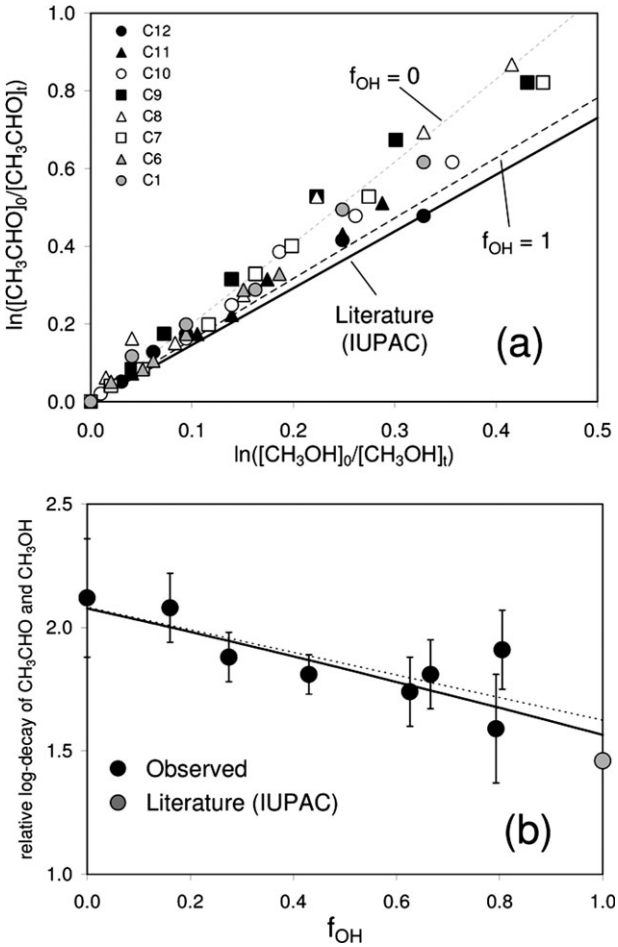

Fig. 6 (a) Relative decay of CH_3CHO and CH_3OH in experiments in 700 Torr of air with $[CH_3OH]_0/[CH_3CHO]_0 \approx 7$, and with benzene added to the system at pressures up to *ca.* 1 Torr (see Table 4). The solid line represents the relative decay by reaction with Cl, based on IUPAC recommended rate coefficients (Atkinson *et al.*,[21]). The dotted and dashed lines are the results of simulations using the mechanism in Table 3 with $k_{3c}/k_3 = 0.43$, for extreme values of f_{OH} (see text); (b) Slopes of regression plots for experiments in panel (a) as a function of f_{OH}. Literature slope is displayed at $f_{OH} = 1$ (*i.e.* the notional absence of OH) for comparison. Solid line is the simulated variation, with $k_{3c}/k_3 = 0.43$. Dotted line is a regression of the experimental points.

as follows,

$$CH_3O_2 + CH_3C(O)O_2 \rightarrow CH_3O + CH_3C(O)O + O_2 \quad (26)$$

$$CH_3O_2 + CH_3O_2 \rightarrow CH_3O + CH_3O + O_2 \quad (27)$$

$$CH_3O + O_2 \rightarrow CH_2O + HO_2 \quad (28)$$

such that the "permutation" reactions of the three peroxy radicals occur in the system under steady state photolysis conditions. As a result, reaction with HO_2 radicals makes a reduced, but still significant, contribution to $CH_3C(O)O_2$ removal, even when CH_3OH is absent.

Fig. 7 shows the dependence of the limiting phenol yield (*i.e.* the OH formation diagnostic) on the precursor reagent concentration ratio. The yield remains approximately constant at *ca.* 0.22 from the high end of the range down to $[CH_3OH]_0/[CH_3CHO]_0 \approx 5$, but decreases at lower ratios to a value at zero $[CH_3OH]$ which is about one third of the high ratio limit. As also shown in the figure, the relative dependence of the limiting phenol yield is similar to that observed for $CH_3C(O)OOH$, indicating that the yields of $CH_3C(O)OOH$ and OH are broadly correlated for the complete range of conditions. It is also noted that the relative dependence is consistent with that reported previously for $CH_3C(O)OOH$ by Crawford *et al.*,[12] based on experiments in the same chamber as used in the present study although, as discussed by Hasson *et al.*,[8] the absolute yields are different due to calibration errors in the Crawford *et al.* study. Given that $CH_3C(O)OOH$ is a well-established product of the reaction of $CH_3C(O)O_2$ with HO_2 (*via* reaction channel (3a)), with no other known sources in the system, the correlation in Fig. 7 provides further support that a major contribution to OH radical formation is made by the reaction of $CH_3C(O)O_2$ with HO_2 (*via* reaction channel (3c)).

3.3.2 Numerical simulation of the system. The above determination of the OH yield at the high end of the considered $[CH_3OH]_0/[CH_3CHO]_0$ range therefore provides an initial estimate of the branching ratio, k_{3c}/k_3. It is recognised, however, that there are a number of complications in the system which preclude such a direct determination of k_{3c}/k_3, namely: (i) a contribution to OH formation results from the $HOCH_2O_2$ chemistry described in Section 3.2; (ii) it is likely that CH_3CHO is removed partially *via* reaction with HO_2 under the experimental conditions; and (iii) although $CH_3C(O)O_2$ reacts mainly with HO_2, a small but significant contribution to

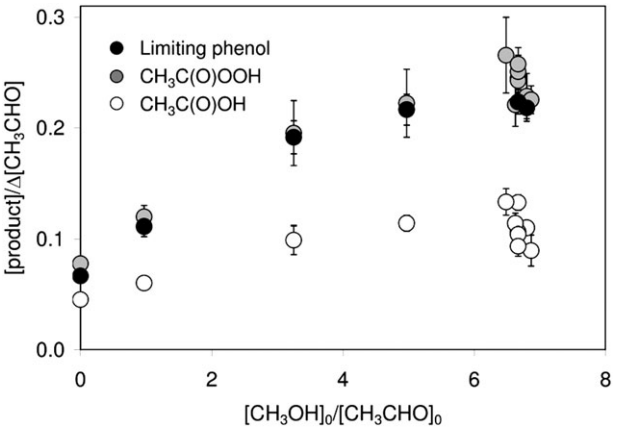

Fig. 7 Variation of the limiting phenol yield and the yields of $CH_3C(O)OOH$ and $CH_3C(O)OH$ with $[CH_3OH]_0/[CH_3CHO]_0$. The limiting phenol yield is the yield of phenol that would result if all OH reacts with benzene, and is determined from the measured yields given in Table 4, divided by f_{OH}. To minimise the extent of correction, phenol data are shown only for experiments with high values of f_{OH}, which lie in the range 0.794–0.843 (experiments C1, C2, C3, C4, C5 and C12). For clarity, displayed error bars are one standard deviation.

$CH_3C(O)O_2$ removal results from its self-reaction and its reactions with CH_3O_2 and $HOCH_2O_2$ (and $CH_3CH(OH)O_2$) under the steady-state photolysis conditions. The system was therefore fully characterised by simulation using the detailed explicit mechanism in Table 3, which allows all these factors to be taken into account.

The value of k_{3c}/k_3 was initially determined from simulations of experiments with $[CH_3OH]_0/[CH_3CHO]_0 \approx 7$ (see Fig. 8a). The value of k_{3c}/k_3 was varied to optimise the agreement between simulated and observed phenol concentrations for $\leq$25% consumption of CH_3CHO. For this procedure, the balance of the reaction was split between channels (3a) and (3b) in a 3:1 ratio, in general accordance with the literature, although sensitivity tests demonstrated that the assessment of channel (3c) was insensitive to this ratio. This provided an optimised value of $k_{3c}/k_3 = 0.43 \pm 0.10$, where the error limits include a 10% contribution from possible systematic errors. On the basis of these simulations, reaction (3c) accounted for 70% of integrated OH formation at $\leq$25% consumption of CH_3CHO, with the balance mainly due to reaction (17c). The similarity of the derived branching ratio with the direct estimate above results from the compensating influences of partial removal of CH_3CHO *via* reaction with HO_2 (discussed below) and partial removal of $CH_3C(O)O_2$ by reactions other than reaction (3). Accordingly, *ca.* 70% of $CH_3C(O)O_2$ was simulated to react with HO_2 (reaction (3)), *ca.* 17% *via* its self reaction (reaction (25)), with the balance *via* reactions with the other RO_2 radicals in the system. The results in Fig. 8b demonstrate that use of the branching ratio $k_{3c}/k_3 = 0.43$ in the mechanism in Table 3 also allows a consistent description of the observed variation of phenol formation with $[CH_3OH]_0/[CH_3CHO]_0$.

The simulated relative contributions of the three removal routes for CH_3CHO (*i.e.* with Cl, OH and HO_2) in the $[CH_3OH]_0/[CH_3CHO]_0 \approx 7$ experiments varied with the quantity of benzene in the system, owing mainly to the

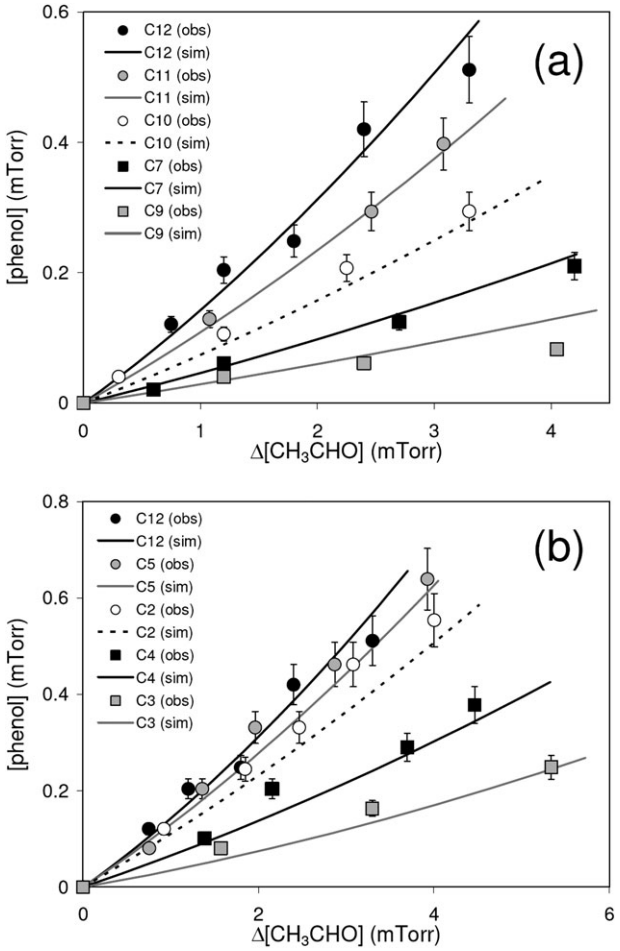

Fig. 8 Observed and simulated formation of phenol relative to CH_3CHO lost during selected $Cl_2/CH_3CHO/CH_3OH$/benzene/air photolysis experiments. The displayed simulations were carried out using the mechanism in Table 3 with an optimised value of $k_{3c}/k_3 = 0.43$. Panel (a) shows results for experiments with $[CH_3OH]_0/[CH_3CHO]_0 \approx 7$, with benzene added to the system at pressures up to *ca.* 1 Torr. Panel (b) shows results for experiments with *ca.* 1 Torr benzene, for $[CH_3OH]_0/[CH_3CHO]_0$ over the range 0–*ca.* 7. Phenol data have been corrected for dark removal (see text).

scavenging of OH, formalised by the parameter f_{OH} defined above. Thus, in the absence of benzene ($f_{OH} = 0$), CH_3CHO removal by reaction with Cl, OH and HO_2 accounted for 68.3%, 25.1% and 6.6%†, respectively. At the highest benzene concentration employed (corresponding to $f_{OH} \approx 0.8$), removal by reaction with Cl, OH and HO_2 accounted for 86.4%, 6.3% and 7.3%†, respectively. A (notional) simulation with sufficient benzene to scavenge all OH radicals ($f_{OH} = 1$) resulted in 92.5% and 7.5%† of CH_3CHO removal by reaction with Cl and HO_2, respectively. These simulations with $k_{3c}/k_3 = 0.43$ therefore allow a good quantitative interpretation of the observed relative removal rates of CH_3CHO and CH_3OH in Fig. 6, providing additional support for the simulated

† This figure specifies the *net* removal of CH_3CHO following its reversible reaction with HO_2. As indicated in Table 3, $CH_3CH(OH)O_2$ is formed in equilibrium with CH_3CHO and HO_2, such that reaction of $CH_3CH(OH)O_2$ with HO_2 and the other peroxy radicals in the system leads to irreversible loss of CH_3CHO.

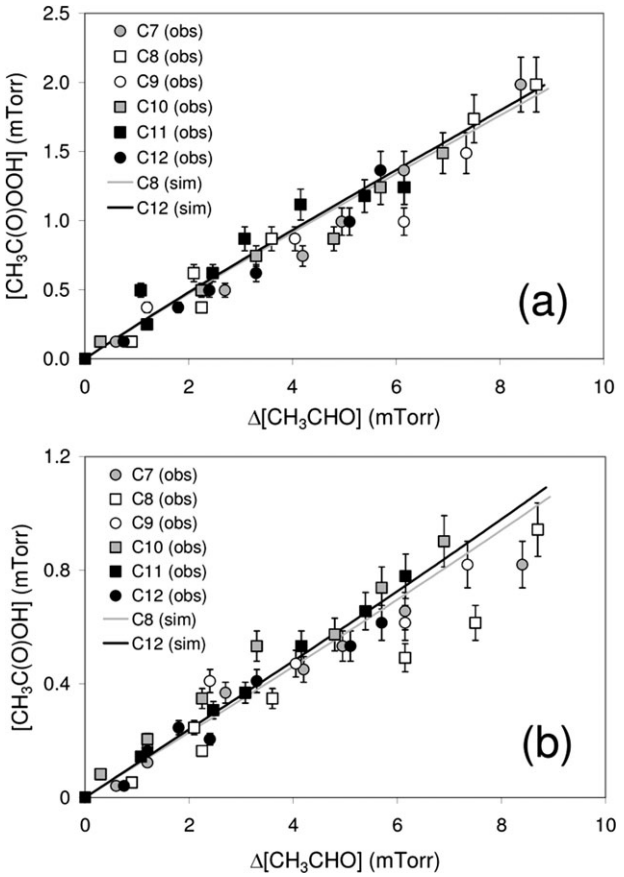

Fig. 9 Observed and simulated formation of (a) $CH_3C(O)OOH$ and (b) $CH_3C(O)OH$ relative to CH_3CHO lost during $Cl_2/CH_3CHO/CH_3OH$/benzene/air photolysis experiments with $[CH_3OH]_0/[CH_3CHO]_0 \approx 7$ and benzene in the range 0–*ca.* 1 Torr. The displayed simulations were carried out using the mechanism in Table 3 with optimised values of $k_{3a}/k_3 = 0.38$ and $k_{3b}/k_3 = 0.12$. The simulations showed a very subtle sensitivity to the presence of benzene, such that the results are shown only for the extreme cases C8 (no benzene) and C12 (1010 mTorr benzene).

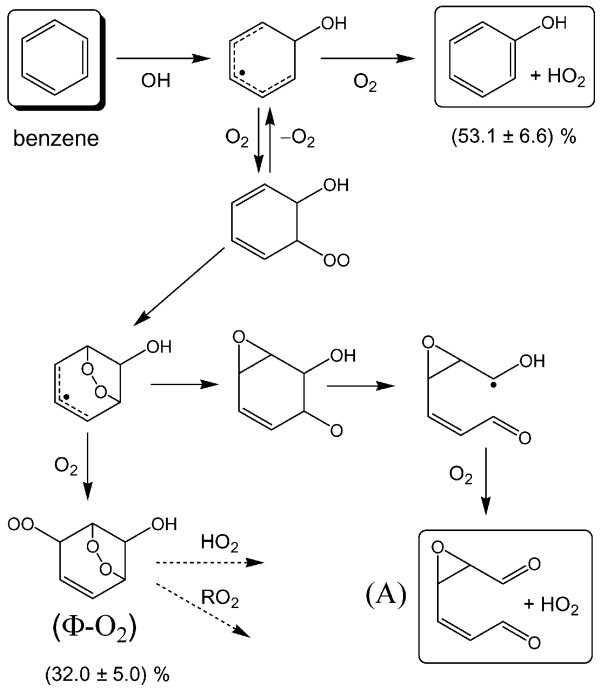

Fig. 10 Schematic representation of the OH-initiated oxidation of benzene. The displayed yield of phenol and HO_2 is from Volkamer *et al.*,[19] and that of the complex peroxy radical (Φ-O_2) is based on the glyoxal yield reported by Volkamer *et al.*[37] (see text). The balance of the reaction is currently believed to lead to the formation of unsaturated epoxy-dicarbonyl products, represented by the displayed route to product (A) (*e.g.*, see discussion in Jenkin *et al.*,[38])

magnitude of OH formation. The general trend in Fig. 6b therefore results from the diminishing preferential removal of CH_3CHO by reaction with OH as f_{OH} increases, and the minor removal of CH_3CHO *via* reaction with HO_2 accounts for the extrapolated limiting relative rate at $f_{OH} = 1$ being slightly greater than the literature ratio of the Cl atom rate coefficients.

The organic products of the other channels of reaction (3), $CH_3C(O)OOH$ and $CH_3C(O)OH$ were also detected and quantified, and their formation relative to CH_3CHO removed in the $[CH_3OH]_0/[CH_3CHO]_0 \approx 7$ experiments is shown in Fig. 9. Because the experimental conditions were optimised for the investigation of channel (3c), comparatively low concentrations of CH_3CHO were used (*i.e.* typically a factor of 2–15 lower than used in the study of Crawford *et al.*[12] in the same chamber), so that it was possible to employ sufficiently high [benzene]/$[CH_3CHO]$ ratios without saturating large portions of the spectral range. In consequence, the yields of $CH_3C(O)OOH$ and $CH_3C(O)OH$ display a degree of scatter, although the composite dataset provides a reasonable quantification of their formation. Values of k_{3a}/k_3 and k_{3b}/k_3 were determined from simulations in which the values of the respective branching ratios were varied to optimise the agreement between simulated and observed $CH_3C(O)OOH$ and $CH_3C(O)OH$ for the complete series of experiments. For this procedure, k_{3c}/k_3 was fixed at 0.43, and compensating changes were made to the branching ratio not being optimised (*i.e.* k_{3b}/k_3 when optimising k_{3a}/k_3, and *vice versa*) to account for the balance of the reaction. This provided optimised values of $k_{3a}/k_3 = 0.38 \pm 0.13$ and $k_{3b}/k_3 = 0.12 \pm 0.04$ (see Fig. 9) which, for consistency with the determination of k_{3c}/k_3, were based on optimisation to data corresponding to $\leq$ *ca.* 25% consumption of CH_3CHO (*i.e. ca.* 4 mTorr in most experiments).

3.4 Assessment of potential impacts of other oxidation pathways for benzene

Because the formation of phenol from the OH-initiated oxidation of benzene accounts for only about half of its removal, it is also necessary to consider any interferences which might result from the other oxidation pathways. Salient features of the OH-initiated oxidation chemistry are illustrated in Fig. 10, demonstrating the formation of phenol and HO_2 *via* reactions (12) and (13), and the alternative formation and subsequent fates of the hydroxycyclohexadienyl peroxy radical which is produced from the sequential addition of OH and O_2 to benzene. Current understanding of the oxidation mechanism indicates that the cyclisation of the peroxy radical, followed by

addition of a second O_2 (to form the complex peroxy radical denoted Φ-O_2), represents the majority of the remainder of the reaction (*e.g.*, Volkamer *et al.*[19,34,37]); with a small additional route forming an unsaturated epoxydicarbonyl product and HO_2 usually assumed to account for the balance of the reaction (*e.g.*, Jenkin *et al.*[38]). The displayed yield of Φ-O_2, (32.0 ± 5.0)%, is based on the yield of glyoxal (CH(O)CHO) reported by Volkamer *et al.*,[37] glyoxal being produced following the reaction of Φ-O_2 with NO in their system, *e.g.*,

$$\Phi\text{-}O_2 + NO \rightarrow \Phi\text{-}O + NO_2 \quad (29)$$

$$\Phi\text{-}O \rightarrow CH(O)CH{=}CHCHO + CH(O)CHOH \quad (30)$$

$$CH(O)CHOH + O_2 \rightarrow CH(O)CHO + HO_2 \quad (31)$$

In the current experiments, Φ-O_2 can react with either HO_2 or organic peroxy radicals such as $CH_3C(O)O_2$ and CH_3O_2 (collectively denoted RO_2 in Fig. 10). Under the high $[CH_3OH]_0/[CH_3CHO]_0$ conditions used to quantify the branching ratios of reactions (3) above, however, it is reasonable to assume that Φ-O_2 reacts mainly with HO_2. Although formation of a hydroperoxide product (reaction (32a)) is likely to occur, the existence of a radical-forming channel (32b), analogous to reaction (3c) for $CH_3C(O)O_2$, would lead to regeneration of OH radicals and therefore additional phenol formation:

$$\Phi\text{-}O_2 + HO_2 \rightarrow \Phi\text{-}OOH + O_2 \quad (32a)$$

$$\Phi\text{-}O_2 + HO_2 \rightarrow \Phi\text{-}O + OH + O_2 \quad (32b)$$

An upper limit to the resultant interference can thus be estimated by assuming that Φ-O_2 reacts exclusively with HO_2, and that the reaction proceeds *via* channel (32b). Under these circumstances, the total yield of phenol (Y_{phenol}) resulting from the initial attack of OH on benzene would be given by,

$$Y_{phenol} = \alpha + \alpha\beta f_{OH} + \alpha(\beta f_{OH})^2 + \alpha(\beta f_{OH})^3 + \ldots + \quad \text{(i)}$$

where α denotes the primary phenol yield, β the yield of regenerated OH and f_{OH} the fraction of OH radicals reacting with benzene in the system, as defined above. Y_{phenol} is therefore the sum of a standard geometric progression, which can be shown to be given by,

$$Y_{phenol} = \alpha/(1 - (\beta f_{OH})) \quad \text{(ii)}$$

such that the actual yield would be greater than the primary yield (α) by a factor of $1/(1 - (\beta f_{OH}))$. With the upper limit value of $\beta = 0.32$, and $f_{OH} = 0.8$ (typical for the high $[CH_3OH]_0/[CH_3CHO]_0$ experiments in the presence of *ca.* 1 Torr benzene), the actual yield of phenol would thus be elevated by a factor of 1.34, and it would be necessary to reduce the value of k_{3c}/k_3 derived above by the same factor (*i.e.*, from 0.43 to 0.32). Noting that this result would still indicate a significant participation of reaction channel (3c), the observed results are nonetheless inconsistent with an interference of this magnitude. First, this degree of OH regeneration would lead to notable upward curvature in the phenol yield data presented in Fig. 5, because the slope of the plot would depend on f_{OH}. Secondly, the significant regeneration of OH by reaction (32b) would also result in the formation of glyoxal (*via* subsequent reactions (23) and (24)), in a comparable yield to phenol. No evidence for the formation of glyoxal was observed, and an upper limit of 5% can be placed on its yield. On the basis of this upper limit, and the level of curvature which could be supported by the data in Fig. 5, we place an upper limit of 0.16 on the value of β, consistent with $k_{32b}/k_{32} \leq 0.5$. Adopting this upper limit would lead to only a small reduction in the derived value of k_{3c}/k_3 to 0.37, which is well within the error bounds of the determination reported above, which therefore remains our recommended value.

3.5 Comparison with previous determinations

The results presented above provide strong evidence for a significant contribution from the radical-forming channel of the $CH_3C(O)O_2 + HO_2$ reaction. Although absolute confirmation would ideally require direct observation of OH formation, it is difficult to find an alternative explanation for the precise dependence of the phenol yield on the concentration of benzene and on $[CH_3OH]_0/[CH_3CHO]_0$, and its strong correlation with the yield of $CH_3C(O)OOH$. The value of the branching ratio, $k_{3c}/k_3 = 0.43 \pm 0.10$, determined in the present study agrees well with that reported by Hasson *et al.* (2004), $k_{3c}/k_3 = 0.40 \pm 0.16$, which was based on the observed variation of the yields of a number of oxidation products (in particular CH_3OOH) with $[CH_3OH]_0/[CH_3CHO]_0$ using FTIR/HPLC. As pointed out by Hasson *et al.*,[8] these values are also consistent with the results of Niki *et al.*,[10] who reported yields of CH_3OOH approaching 50%, relative to CH_3CHO removed, at high $[HCHO]_0/[CH_3CHO]_0$ in their FTIR product study of the Cl atom initiated oxidation of CH_3CHO/HCHO/air mixtures (HCHO being the HO_2 precursor in their system).

The present results do not support the value of $k_{3c}/k_3 < 0.1$ reported by Le Crane *et al.*[15] As indicated above, their upper limit was determined partly from a re-evaluation of the results of the flash photolysis/UV absorption kinetics study of Tomas *et al.*[14] from the same laboratory, and partly on the basis of new experiments in which benzene was added to the system to scavenge OH radicals. However, scrutiny of the reported information suggests that the results may have been misinterpreted, allowing greater values of k_{3c}/k_3 to be supported. Our reasons for this assertion are now given.

In the re-evaluation of the Tomas *et al.*[14] data, the simulation of the system was initially constrained to the branching ratios reported by Hasson *et al.*[8] for channels (3a), (3b) and (3c) (0.40 ± 0.16, 0.20 ± 0.08 and 0.40 ± 0.16, respectively) and to the absorption cross sections recommended for the peroxy radicals by Tyndall *et al.*;[3] although variation of the parameters within the quoted uncertainty limits was not considered. The value of k_3 was re-optimised using data measured at 207 nm (where both $CH_3C(O)O_2$ and HO_2 absorb strongly), logically resulting in a notable increase in the rate coefficient (in response to the regeneration of the radicals following reactions (16) and (24)) and a very good fit to the observed decay in absorption. However, use of the same parameters resulted in a consistent (comparatively small) overestimate of the observed absorptions at 240 nm, on

timescales up to *ca.* 400 ms. To address this shortcoming, the value of k_{3c}/k_3 was reduced to close to zero whilst making a compensating increase in the value of k_{3a}/k_3 and optimising k_3. The value of k_{3b}/k_3 was simultaneously optimised at 0.20 ± 0.01 on the basis of the residual absorption at 240 nm at long timescales, which was due to O_3. However, the use of lower values of k_{3b}/k_3, in conjunction with $k_{3c}/k_3 = 0.4$, was not considered, even though a reduction in the O_3 yield is a direct and logical way to solve the discrepancy at 240 nm. Because the associated regeneration of $CH_3C(O)O_2$ and HO_2 in the system if channel (3c) is significant must result in additional O_3 formation, it is clear that a good fit to the 240 nm data could never be achieved whilst k_{3b}/k_3 was constrained to the value of 0.2 (*i.e.*, the value derived with the assumption that $k_{3c}/k_3 \approx 0$). It is highly probable that use of a lower value of k_{3b}/k_3, in conjunction with $k_{3c}/k_3 \approx 0.4$, would allow acceptable fits to the 240 nm data. In this respect, direct measurements of k_{3b}/k_3 based on yields of $CH_3C(O)OH$ and O_3 relative to CH_3CHO removed, in the studies of Niki *et al.*,[10] Crawford *et al.*[12] and the present study, are consistent with a branching ratio in the region of 0.1–0.15. Values towards the high end of this range are also compatible with the determination of Hasson *et al.*,[8] within the quoted uncertainty limits. It is also noted that uncertainties in the peroxy radical absorption cross sections must also afford some level of tolerance in fitting the composite absorptions, such that the lack of a precise fit does not necessarily indicate erroneous kinetic parameters.

In the new kinetics experiments, Le Crane *et al.*[15] investigated the potential formation of the hydroxycyclohexadienyl radical (HOC_6H_6) when high concentrations of benzene were added to the system to scavenge OH radicals. Kinetic absorption traces were measured at 290 nm, where the HOC_6H_6 radical absorbs strongly, and the system was simulated with a mechanism which included a detailed representation of the formation and removal of the radical. The simulated traces were found to overestimate the observed small absorptions over a 10 ms period when k_{3c}/k_3 was set to a value of 0.4, and improved fits were obtained by decreasing the branching ratio to <0.1. It is difficult to appraise fully the results of this analysis, because the information given in the paper is necessarily limited. Several rate coefficients are assigned wide ranges in the mechanism, but no indication of the values actually used in the simulations presented in the paper is given. However, there also appears to be a notable omission from the applied reaction mechanism, namely the irreversible component of the reaction of HOC_6H_6 with O_2. This reaction leads to the formation of phenol and other products (see Fig. 10), and is likely to be the major loss process controlling the concentration of HOC_6H_6 in the system at the high O_2 concentrations employed (0.95 atm). Based on the characterisation of the OH + benzene system reported previously by workers in the same group,[39,40] the corresponding lifetime of HOC_6H_6 with respect to this reaction is of the order of 0.2 ms. In the absence of this reaction, the simulated HOC_6H_6 is removed as a result of radical–radical reactions in the system, and is therefore second order in nature. Accordingly, simulations performed here using the mechanism and conditions reported by Le Crane *et al.*[15] demonstrated that incorporation of the irreversible reaction with O_2 has a major influence on the simulated time dependence of the HOC_6H_6 concentration, and the associated absorption at 290 nm. The peak concentration generated soon after the flash was reduced by *ca.* 10%, and the concentration decayed away with a time constant of the order of 1 ms, such that the concentrations after 5 and 10 ms were lower by a factors of *ca.* 20 and 400, respectively, than simulated with the irreversible component of the reaction omitted. The result therefore strongly suggests that the simulation of the 290 nm experimental absorption profile reported by Le Crane *et al.*[15] would be substantially improved in both shape and magnitude, such that the data can support a significant contribution from the radical-forming channel of the $CH_3C(O)O_2 + HO_2$ reaction. It is also probable that characterisation of HOC_6H_6 formation, and confirmation of the participation of channel (3c), could be facilitated by carrying out experiments at lower O_2 concentrations.

The values of $k_{3a}/k_3 = 0.38 \pm 0.13$ and $k_{3b}/k_3 = 0.12 \pm 0.04$, reported above on the basis of the formation of $CH_3C(O)OOH$ and $CH_3C(O)OH$, can be used to derive a value of $k_{3a}/k_{3b} \approx 3$. This is in reasonable accord with values of k_{3a}/k_{3b}, lying in the range 2–3, which can derived from studies in which branching ratios for both channels have been quantified.[8,10,11]

4. Conclusions and atmospheric implications

The results presented above for $CH_3C(O)O_2$ and $HOCH_2O_2$, and previously by Hasson *et al.*[8] for $CH_3C(O)O_2$, suggest that the reaction with HO_2 is a less efficient chain terminating process for selected oxygenated RO_2 radicals in the atmosphere than previously thought, which may alter our assessment of processes controlling ambient radical concentrations under NO_x-limited conditions. The results of Hasson *et al.*[8] suggest that the reaction of $CH_3C(O)CH_2O_2$ with HO_2 has an even lower terminating fraction than reaction (3), and it is therefore possible that the reactions of HO_2 with acyl, α-carbonyl and α-hydroxy RO_2 radicals in general may be significantly propagating. It is therefore important that the possible participation of propagating channels is investigated for these and other RO_2 radical classes, in particular the β-hydroxyperoxy radicals generated from reactions of OH with alkenes and dienes, most notably isoprene and monoterpenes. Direct detection of the radical products (*e.g.*, OH), and studies as a function of temperature would also be valuable.

Acknowledgements

MEJ acknowledges the UK Natural Environment Research Council, NERC, for support *via* a Senior Research Fellowship (NE/D008794/1).

References

1 T. J. Wallington, P. Dagaut and M. J. Kurylo, *Chem. Rev.*, 1992, **92**, 667.

2 P. D. Lightfoot, R. A. Cox, J. N. Crowley, M. Destriau, G. D. Hayman, M. E. Jenkin, G. K. Moortgat and F. Zabel, *Atmos. Environ.*, 1992, **26A**, 1805.
3 G. S. Tyndall, R. A. Cox, C. Granier, R. Lesclaux, G. K. Moortgat, M. J. Pilling, A. R. Ravishankara and T. J. Wallington, *J. Geophys. Res. D*, 2001, **106**, 12157.
4 M. E. Jenkin and K. C. Clemitshaw, *Atmos. Environ.*, 2000, **34**, 2499.
5 T. J. Wallington, *J. Chem. Soc., Faraday Trans.*, 1991, **87**, 2379–2382.
6 M. Spittler, I. Barnes, K. H. Becker and T. J. Wallington, *Chem. Phys. Lett.*, 2000, **321**, 57.
7 M. J. Elrod, D. L. Ranschaert and N. J. Schneider, *Int. J. Chem. Kinet.*, 2001, **33**, 363.
8 A. S. Hasson, G. S. Tyndall and J. J. Orlando, *J. Phys. Chem. A*, 2004, **108**, 5979.
9 A. S. Hasson, K. T. Kuwata, M. C. Arroyo and E. B. Petersen, *J. Photochem. Photobiol., A*, 2005, **176**, 218.
10 H. Niki, P. D. Maker, C. M. Savage and L. P. Breitenbach, *J. Phys. Chem.*, 1985, **89**, 588.
11 O. Horie and G. K. Moortgat, *J. Chem. Soc., Faraday Trans.*, 1992, **88**, 3305.
12 M. A. Crawford, T. J. Wallington, J. J. Szente, M. M. Maricq and J. S. Francisco, *J. Phys. Chem. A*, 1999, **103**, 365.
13 G. K. Moortgat, B. Veyret and R. Lesclaux, *Chem. Phys. Lett.*, 1989, **160**, 443.
14 A. Tomas, E. Villenave and R. Lesclaux, *J. Phys. Chem. A*, 2001, **105**, 3505.
15 J. P. Le Crane, M. T. Rayez, J. C. Rayez and E. Villenave, *Phys. Chem. Chem. Phys.*, 2006, **8**, 2163.
16 T. J. Wallington and S. M. Japar, *J. Atmos. Chem.*, 1989, **9**, 399.
17 O. Sokolov, M. D. Hurley, T. J. Wallington, E. W. Kaiser, J. Platz, O. J. Nielsen, F. Berho, M. T. Rayez and R. Lesclaux, *J. Phys. Chem. A*, 1998, **102**, 10671.
18 J. G. Calvert, R. Atkinson, K. H. Becker, R. M. Kamens, J. H. Seinfeld, T. J. Wallington and G. Yarwood, *The mechanisms of atmospheric oxidation of aromatic hydrocarbons*, Oxford University Press, New York, ISBN 0-19-514628-X, 2002.
19 R. Volkamer, B. Klotz, I. Barnes, T. Imamura, K. Wirtz, N. Washida, K. H. Becker and U. Platt, *Phys. Chem. Chem. Phys.*, 2002, **4**, 1598.
20 J. Platz, O. J. Nielsen, T. J. Wallington, J. C. Ball, M. D. Hurley, A. M. Straccia, W. F. Schneider and J. Sehested, *J. Phys. Chem. A*, 1998, **102**, 7964.
21 R. Atkinson, D. L. Baulch, R. A. Cox, J. N. Crowley, R. F. Hampson, R. G. Hynes, M. E. Jenkin, M. J. Rossi and J. Troe, *Atmos. Chem. Phys.*, 2006, **6**, 3625.
22 R. Buth, K. Hoyermann and J. Seeba, *25th Symposium on Combustion*, The Combustion Institute, 1994, 841.
23 Z. Tao and Z. Li, *Int. J. Chem. Kinet.*, 1999, **31**, 65.
24 F. Su, J. G. Calvert and J. H. Shaw, *J. Phys. Chem.*, 1979, **83**, 3185.
25 H. Niki, P. D. Maker, C. M. Savage and L. P. Breitenbach, *Chem. Phys. Lett.*, 1980, **72**, 72.
26 B. Veyret, R. Lesclaux, M. T. Rayez, J. C. Rayez, R. A. Cox and G. K. Moortgat, *J. Phys. Chem.*, 1989, **93**, 2368.
27 J. P. Burrows, G. K. Moortgat, G. S. Tyndall, R. A. Cox, M. E. Jenkin, G. D. Hayman and B. Veyret, *J. Phys. Chem.*, 1989, **93**, 2375.
28 R. Atkinson, D. L. Baulch, R. A. Cox, J. N. Crowley, R. F. Hampson, R. G. Hynes, M. E. Jenkin, M. J. Rossi and J. Troe, *Atmos. Chem. Phys.*, **4**, 1461.
29 B. Veyret, P. Roussel and R. Lesclaux, *Int. J. Chem. Kinet.*, 1984, **16**, 1599.
30 J. Orlando, B. Nozière, G. Tyndall, G. Orzechowska, S. Paulson and Y. Rudich, *J. Geophys. Res.*, **105**, 11561.
31 M. E. Jenkin, M. P. Sulbaek Andersen, M. D. Hurley, T. J. Wallington, F. Taketani and Y. Matsumi, *Phys. Chem. Chem. Phys.*, 2005, **7**(6), 1194.
32 E. S. C. Kwok and R. Atkinson, *Atmos. Environ.*, 1995, **29**, 1685.
33 S. M. Saunders, M. E. Jenkin, R. G. Derwent and M. J. Pilling, *Atmos. Chem. Phys.*, 2003, **3**, 161–180.
34 R. Volkamer, U. Platt and K. Wirtz, *J. Phys. Chem. A*, 2001, **105**, 7865.
35 A. Bierbach, I. Barnes, K. H. Becker and E. Wiesen, *Environ. Sci. Technol.*, 1994, **28**, 715.
36 G. L. Vaghjiani and A. R. Ravishankara, *J. Phys. Chem.*, 1989, **93**, 1948.
37 R. Volkamer, P. Spietz, J. Burrows and U. Platt, *J. Photochem. Photobiol., A*, 2005, **172**, 35.
38 M. E. Jenkin, S. M. Saunders, V. Wagner and M. J. Pilling, *Atmos. Chem. Phys.*, 2003, **3**, 181.
39 D. Johnson, S. Raoult, M. T. Rayez, J. C. Rayez and R. Lesclaux, *Phys. Chem. Chem. Phys.*, 2002, **4**, 4678.
40 S. Raoult, M. T. Rayez, J. C. Rayez and R. Lesclaux, *Phys. Chem. Chem. Phys.*, 2004, **6**, 2245.

